To appear in Acta Materialia, **48**, [18-19], 4425-4438 (2000)

Joining of Alumina *via* Copper/Niobium/Copper Interlayers

Robert A. Marks, Daniel R. Chapman, David T. Danielson and Andreas M. Glaeser

Department of Materials Science and Mineral Engineering,
University of California
&
Center for Advanced Materials
Lawrence Berkeley National Laboratory, Berkeley, CA 94720

Abstract

Alumina has been joined at 1150°C and 1400°C using multilayer copper/niobium/copper interlayers. Four-point bend strengths are sensitive to processing temperature, bonding pressure, and furnace environment (ambient oxygen partial pressure). Under optimum conditions, joints with reproducibly high room temperature strengths (≈240 ± 20 MPa) can be produced; most failures occur within the ceramic. Joints made with sapphire show that during bonding an initially continuous copper film undergoes a morphological instability, resulting in the formation of isolated copper-rich droplets/particles at the sapphire/interlayer interface, and extensive regions of direct bonding between sapphire and niobium. For optimized alumina bonds, bend tests at 800°C-1100°C indicate significant strength is retained; even at the highest test temperature, ceramic failure is observed. Post-bonding anneals at 1000°C in vacuum or in gettered argon were used to assess joint stability and to probe the effect of ambient oxygen partial pressure on joint characteristics. Annealing in vacuum for up to 200 h causes no significant decrease in room temperature bend strength or change in fracture path. With increasing anneal time in a lower oxygen partial pressure environment, the fracture strength decreases only slightly, but the fracture path shifts from the ceramic to the interface.

Introduction

Ceramic-metal interfaces are a critical feature in many materials systems, and processing of these interfaces is fundamental to fabrication of a wide range of materials and devices. Of the numerous methods available for ceramic-ceramic and ceramic-metal joining, solid-state diffusion bonding and reactive metal brazing have been most heavily investigated for producing reliable joints for demanding high-stress, high-temperature applications [1-5]. Diffusion bonding and brazing have unique advantages, but also liabilities that increase in number and severity as processing temperatures are increased. Since diffusion bonding (brazing) temperatures generally approach (exceed) the intended use temperature, microstructural degradation during joining becomes an increasingly important issue as joining temperatures increase. Greater attention must also be paid to chemical compatibility of the components to be joined with one another and the joining media. Incompatibilities that are absent or mitigated by sluggish reaction kinetics at low temperature manifest themselves more obviously when joints are produced at elevated temperature. As a result of these complications, the technology for producing refractory joints is not as well developed as that for low-temperature joints.

Over the past thirty years, numerous approaches designed to develop refractory joints by means of low-temperature processes have been explored. Efforts were made to extent transient liquid phase (TLP™) methods for joining nickel-base superalloys to the joining of silicon nitride [6-13] and silicon carbide [14, 15] ceramics. Multilayer interlayers combining lower and higher melting point metals that would homogenize by solid-state diffusion were proposed as alternatives to the homogeneous metallic interlayers normally used for solid-state diffusion bonding [16]. Joining methods utilizing multilayer metallic interlayers under conditions where a thin or partial layer of a transient liquid phase forms were also proposed [17, 18]. The partial transient liquid phase (PTLP) method has been used to join oxide [18-23] and nonoxide ceramics [21-26].

Prior work exploring the use of multilayer copper/niobium/copper interlayers for the joining of alumina [20] demonstrated that strong joints could be produced at 1150°C, well below the temperatures normally used for solid-state diffusion bonding of niobium to alumina. The limited solubility and slow

diffusion of copper in niobium prevented disappearance of the liquid phase at the joining temperature. However, it was observed that the initially continuous copper film evolved into discrete copper-rich particles during processing; liquid-phase assisted growth of contact regions between niobium and alumina had apparently occurred. The present work is part of a broader effort to examine the effects of processing conditions on joint properties and to establish fundamental processing-microstructure-property relationships. The results demonstrate that under appropriate conditions, interfacial microstructures that yield reproducible strengths at both room and elevated temperature (800-1100°C) can be attained.

Background

The approach to bonding explored uses a multilayer metallic interlayer. Both of the ceramic surfaces to be joined are coated with a thin cladding layer of a low melting metal, copper in this case. A thick core layer of a high melting point metal, niobium in this study, is inserted between the coated alumina surfaces. At the bonding temperature, 1150°C or 1400°C, the cladding layers melt, while the core layer remains solid. As a result, a thin liquid layer forms between the ceramic and core layer. The sum of the contact angles of the liquid on the ceramic, θ_1, and on the core metal, θ_2, must be less than 180° to promote void filling and thinning of the liquid film. With increasing time at temperature, discrete copper-rich particles, and thus, regions of niobium/alumina and copper/alumina bonding, develop along the alumina/interlayer interface. As a result, the properties of the joined assemblies reflect the properties of niobium/alumina interfaces, copper/alumina interfaces, and the wetting behavior of a copper-rich liquid on both niobium and alumina. Prior work addressing these topics is reviewed.

Prior Work on Niobium/Sapphire Interfaces

The niobium/sapphire system has been a model metal/ceramic system for nearly thirty years due to the excellent thermal expansion match between the two materials, their high melting temperatures, and the absence of severe chemical interaction. The diffusion bonding of these materials, their interfacial structure, chemical compatibility, strength and failure characteristics, and the influence of interfacial impurities have all been examined and reported extensively in the literature.

Diffusion Bonding Conditions and Joint Properties

Diffusion bonding of sapphire or alumina to niobium has been performed over a wide range of time-temperature-bonding load conditions. Generally, for conventional high vacuum (HV; ≈10^{-3} Pa) diffusion bonding, studies have focussed on the temperature range 1500-1950°C, with bonding times of several hours, and a bonding load typically of the order of 10 MPa [27-31]. Bonding temperature reductions of up to 500°C relative to HV bonding can be achieved by the use of ultrahigh vacuum (UHV; ≈10^{-8} Pa) conditions coupled with sputter cleaning of the bonding surfaces [32]. However, in both HV and UHV bonds, fracture energies increase with increasing bonding temperature, a trend attributed to an increase in the area fraction bonded.† As a result, "typical" UHV bonding conditions for niobium/sapphire involve 3 h at 1400°C with an applied load of 10 MPa; these conditions allow the fabrication of well-bonded couples with high fracture energies.

Mechanical tests of both bicrystal joints and polycrystalline niobium/polycrystalline alumina joints have provided fracture energy (G_c) values. Samples in which oriented sapphire and oriented niobium single crystals are bonded show that G_c is very sensitive to the interface crystallography with values ranging from ≈60 [35] to ≈2400 J/m^2 [36] in room temperature tests. For most crystallographies, the failures are interfacial. Bonds involving polycrystals typically undergo interfacial failure, and exhibit either lower fracture energies [37], or fracture energies nearer to the lower bicrystal values [36]. A limited number of strength measurements indicate that joints processed at 1600°C under HV conditions fail at stresses of the order of 100-150 MPa [27, 29].

Dissolution of Alumina; Oxygen and Aluminum Diffusion

Although niobium does not reduce alumina, alumina dissolves at the niobium/alumina interface and both oxygen and aluminum diffuse into the adjoining niobium [28-32, 38, 39]. The equilibrium oxygen levels in initially pure niobium due to alumina dissolution increase with temperature, and are predicted to be of the order of 0.07 at% at 1000°C and ≈1 at% at 1600°C [40] assuming that there is no loss of oxygen or

† The clearest demonstration of this is found in the work of Gibbesch and Elssner [33]. Gibbesch *et al.* [34] have compared the fracture energy of UHV and HV diffusion bonded niobium/alumina joints, and results indicate that equivalent G_c values can be obtained at ≈300°C lower bonding temperature when the UHV environment and sputter cleaning are used. Korn *et al.* cite an ≈200°C reduction in processing temperature when equal bonding pressures are used [35].

aluminum to the ambient. The hardness and yield stress of niobium increase approximately linearly with oxygen content [41],✣ and bonds produced at ≥1600°C (or that use niobium intentionally doped with oxygen [42]) have undesirable properties [29].

Aluminum diffuses substitutionally in niobium, while oxygen diffuses by an interstitial mechanism. At 1000°C and 1400°C, the oxygen diffusivity [43, 44] to aluminum diffusivity [45] ratio is of the order 10^8 to 10^5, respectively, and thus, the relative diffusion distance for oxygen is much greater, especially at lower temperatures. A simplified theoretical model, assuming independent diffusion of aluminum and oxygen within niobium (and no loss of either specie), and no solubility limit for aluminum or oxygen has been developed to predict the compositional profiles of aluminum and oxygen in niobium [46]. Predicted near-interfacial aluminum levels are of the order 10-12 at% over a wide bonding temperature range. Experimental values are a factor of 4-6× lower, largely due to recondensation and precipitation during cooling. Transmission electron microscopy studies [28, 31, 38, 39] show that θ-alumina precipitates can form in the near-interfacial region, and that alumina can also condense at interfacial flaws, with the details of the evolution sensitive to cooling rate [38, 39]. Thermodynamic considerations [47] indicate that the initial oxygen (or aluminum) content of the niobium and the ambient oxygen pressure will have a substantial influence on the dissolution, and thus, the near-grain boundary chemistry during bonding.

Role of Interfacial Impurities

Fracture in niobium/sapphire and niobium/alumina couples is generally interfacial. Thus, impurities that segregate to this interface can affect the resulting fracture strength directly through their effect on interfacial adhesion, and indirectly through the effect of adhesion on plastic dissipation accompanying fracture. Korn *et al.* [35] and Elssner *et al.* [48] examined the influence of interface impurities (Ag, S, Ti) on the fracture energy of UHV bonded niobium/sapphire bicrystals prepared at 1400°C. Submonolayer to nanometer thick layers of silver were found to yield a segregation profile and decrease the fracture energy, G_c. Segregation of sulphur, present as an impurity at a 30 ppm level in the niobium, was

✣ At bonding temperatures above ≈1600°C, the compositions of oxygen-doped niobium samples relax to a near-equilibrium value within typical bonding times, and as a result, the joint properties are "independent" of the initial oxygen level [40]. At lower temperatures, and in other studies, the deleterious role of excessive oxygen levels has been demonstrated clearly [42].

detected at niobium/vapor interfaces after anneals at 1400°C. When foils with sulphur segregant were used to prepare bonds, segregation at the niobium/sapphire interface was negligible, and changes in G_c were small (within experimental error). In contrast, titanium substantially increases G_c; increased interfacial adhesion increases the contribution of plasticity to the work of fracture [48].

Tantalum and oxygen are common impurities in niobium [49]. Tantalum and niobium form complete solid solutions [50], and pure tantalum has a higher surface energy than pure niobium [51]. Thus, tantalum segregation to the surface is expected to be minimal. Oxygen can play multiple roles. It hardens niobium, and thus can reduce the contribution of plasticity to the work of failure. It can segregate to the interface, and influence interfacial adhesion directly (and thereby the plasticity contribution), or it can interact with other impurities [43] and modify their interaction with the niobium/sapphire interface. In the case of niobium/sapphire couples, dissolution of alumina at elevated temperature will add aluminum to the near-interfacial region, and will add to the initial oxygen content. Since oxygen diffusion in niobium is rapid, adjustments of the dissolved oxygen content can occur in regions of the interlayer within a diffusion distance of the surface due to oxygen exchange with the furnace atmosphere.

Elimination of Interfacial Porosity

Gibbesch and Elssner [33] bonded polycrystalline alumina using 2 mm thick, 99.99% pure niobium plates under UHV conditions; the applied pressure was 10 MPa and temperature was varied from 900°C to 1500°C. The area fraction bonded increased with increasing bonding temperature. Plastic deformation of the metal was cited as the dominant mechanism of pore closure at the interface.

The morphological evolution of interfacial porosity during diffusion bonding of niobium and alumina at ≈1450°C was also examined by Reimanis [52]. Sapphire single crystals of two different orientations were bonded to (111)-textured 100-200 μm thick 99.9% pure niobium foils under an applied pressure of 2 MPa, and pore removal at the interface was monitored using optical microscopy. Key findings of the study were that: 1) pore removal proceeded by the growth of highly facetted bonding fronts whose facet structure was related to the orientation of niobium grains, 2) pore removal rates in samples annealed with and without a 2MPa pressure were similar, and 3) that grain boundary grooves in the niobium foil appeared to provide the initial contact points with the sapphire, and played a key role in the development of

new bonded regions. Significant unbonded regions persisted even after 18 h at 1450°C.* It is possible that the combined effects of different niobium thickness, purity, and applied pressure yielded different relative contributions of plasticity and diffusion to pore closure.

Prior Work on Copper/Sapphire Interfaces

Diffusion Bonding Conditions and Joint Properties

Several studies of diffusion bonding of alumina or sapphire using copper interlayers have been reported [32, 33, 53-57]. Most earlier work was conducted under HV conditions, while more recent work has included UHV bonding studies. In general, both HV and UHV bonding temperatures are in the range of 900-1050°C, with bonding times of 0.25-6 h and applied pressures in the range of 1-50 MPa. Several studies examined the effects of bonding temperature, pressure, and time on the area fraction bonded, and/or fracture strength [33, 54, 55, 57]. Results suggest that samples diffusion bonded for periods of a few hours (or less) at temperatures ≥900°C with bonding pressures of ≤10 MPa yield interfaces with high fractions of bonded area [33, 55, 57]; creep of the copper plays a key role in pore removal [53, 55, 57].

Reported strength values for copper/alumina interfaces vary substantially (0 to ≈180 MPa) reflecting differences in processing conditions (interface microstructure), sample geometry, and test method. Measurements by Gibbesch and Elssner [33] suggest that copper/alumina (polycrystal) interfaces have a higher fracture energy than niobium/alumina (polycrystal) interfaces. Bicrystals yield G_c values in the 100-200 J/m^2 range, however, results for only one misorientation have been reported [57]. Fracture energies are particularly sensitive to the presence of oxygen and the formation of phases at the metal/ceramic interface, as will be discussed shortly.

Brazing using Copper-Cuprous Oxide Eutectic and Joint Properties

Most studies of the wetting behavior of "pure" copper on alumina or sapphire indicate obtuse contact angles varying between 110° and 170° [20, 22, 55, 58-64], with more limited evidence suggesting that the contact angle decreases slightly with increasing temperature [59, 62, 63]. The copper-oxygen phase

* Morozumi *et al.* [27] report ≈50% bonded area after 1 h, 8.8 MPa, HV bonding at 1600°C. Turwitt *et al.* [37] report that after a 2 h, 10 MPa HV bonding cycle at 1700°C, ≈10-20% of the interface remains unbonded, suggesting that porosity removal is slow even at substantially higher temperature. In contrast, Gibbesch and Elssner [33] report ≈98% bonded area after 1 h, 10 MPa UHV bonding at 1600°C.

diagram contains a copper-cuprous oxide (Cu_2O) eutectic at 1066°C. As the oxygen solubility limit of copper at 1066°C (≈0.03 at%) is exceeded, a eutectic liquid forms. At higher temperatures (≈1092°-1200°C), oxygen additions can also reduce the contact angle [55, 60, 61, 64], and the wetting behavior of copper on sapphire or alumina has been examined over a wide range of ambient oxygen partial pressure [60, 61, 64]. At sufficiently high oxygen potentials, contact angles as low as ≈10° have been observed [55].

Several investigations have attempted to correlate the mechanical properties of such eutectic-bonded alumina with oxygen content and bonding time [e.g., 65, 66]. Oxygen diffuses rapidly in solid copper [44, 67-70], with reported diffusivities at 1000°C ranging from $\approx 1.4 \times 10^{-5}$ to $\approx 3.1 \times 10^{-5} cm^2/s$, and thus, the oxygen content of copper can be changed by annealing in controlled p_{O_2} environments. Yoshino [65] demonstrated that post-bonding anneals in low p_{O_2} environments degrade the peel strength or push strength, and that anneals in which p_{O_2} is cycled from slightly above to slightly below that required for copper–cuprous oxide equilibrium lead to reproducible and reversible strength changes.

Role of Impurities and Interphases

Studies by Rogers *et al.* [71] and Rühle *et al.* [57] have shown that the levels of dissolved oxygen in even high-purity copper foils are sufficient to induce formation of interphases that impact the mechanical properties of copper/sapphire assemblies. In the work of Rogers *et al.* [71], cuprous oxide needles were present at the interface between 99.95% pure copper and sapphire after 24 h HV diffusion bonding at 1040°C even though the ambient p_{O_2} during diffusion bonding ($\approx 3 \times 10^{-10}$ atm) was well below the copper-cuprous oxide equilibrium p_{O_2} ($\approx 1.6 \times 10^{-6}$ atm).■ The copper foil was found to contain ≈1200 atomic ppm (ppma) oxygen. Rühle *et al.* [57] bonded sapphire to "pure" copper foils and copper foils with 60 ppma dissolved oxygen ($\underline{O}$) under UHV conditions (1 to 3 h, 1.5 MPa bonding pressure, 900°C). Although no interphases were detected when pure copper was used, bonds made with the foils containing 60 ppma $\underline{O}$ yielded a reaction layer of either cuprous oxide or a copper aluminate ($CuAlO_2$) at the copper/sapphire interface. Fracture energy measurement comparisons show that bonds made with copper foils containing 60 ppma $\underline{O}$ yielded approximately four- to seven-fold higher G_c values [57].

■ When bonding experiments were repeated using a graphite enclosure, interfaces free of cuprous oxide needles were obtained.

Controlled p_{O_2} anneals (1000°C, 24 h) were used by Rogers *et al.* [71] to study interphase formation at copper/sapphire interfaces. Sapphire/copper/sapphire diffusion-bonded assemblies were annealed at a p_{O_2} of ≈10^{-7} atm to reduce the cuprous oxide particles, and induce the formation of a copper aluminate at the interface. Subsequent anneals at a p_{O_2} of ≈5×10^{-9} atm reduced both the cuprous oxide and copper aluminate. An anneal at a p_{O_2} of ≈10^{-7} atm reformed copper aluminate. Experiments suggest that nucleation and dissociation of $CuAlO_2$ is sluggish. Subsequent studies by Reimanis *et al.* [72] examined the effect of such post-bonding anneals and interphases on the fracture resistance of bonds. Results suggest that when cuprous oxide is the only interphase at the interface, crack propagation is locally enhanced. In contrast, when $CuAlO_2$ is the only interphase present, crack trapping occurs, and crack propagation is impeded. The fracture energy for interfaces containing $CuAlO_2$ is ≈190 J/m^2, whereas that for crack initiation in interphase-free interfaces is ≈125 J/m^2.

Wetting/Dewetting Studies

Solid Copper on Alumina/Sapphire

The wetting behavior of liquid copper on sapphire has been discussed in a prior section; pure copper liquid does not wet sapphire. Several studies have focussed on the stability of thin solid copper films on sapphire [73, 74]. The results indicate that thin films are morphologically stable to at least 430°C [74], but dewet and evolve into discrete copper clusters when annealed at 650°C at a p_{O_2} consistent with copper-cuprous oxide equilibrium [73]. Measurements of contact angles of solid copper droplets on sapphire indicate the majority lie between 81-90°, and none are greater than 120° [73].

Copper-Niobium Alloys on Alumina

Nakashima has studied the wetting of niobium-saturated copper on alumina and sapphire substrates at 1150°C [22]. Niobium additions result in an immediate (short-term) decrease in the contact angle of liquid copper on polycrystalline alumina from ≈130° (pure copper) to ≈114°. The contact angle continues to decrease with increasing time, reaching values of ≈15° after 6 h.

Copper on Niobium

Three studies of the wetting of copper on niobium have been published, differing in temperature and time span investigated, niobium purity, and the extent to which the role of oxygen was assessed. The sessile drop measurements of DeLima *et al.* [75] used 99.9% pure niobium single crystals and polycrystals, as well as polycrystalline niobium doped with 1.5 and 6.5 at% oxygen, and 99.999% pure copper. Acute contact angles were obtained in all samples after 5 min at all temperatures from 1090°C (38–85°) to 1300°C (0–59°) with the highest values corresponding to niobium doped with 6.5 at% oxygen, and the lowest values for material processed in H_2:10 vol ppm H_2O atmosphere. At fixed temperature and atmosphere, (100) and (110) single crystals and polycrystalline samples showed distinct wetting behaviors. Hodkin *et al.* [51] measured contact angles and dihedral angles for spectroscopically pure copper on two different ≈99.7% pure niobium polycrystalline substrates at 1500°C. The reported contact angle for copper on niobium after 120 h is <3°, and is consistent with the general data trend in this system towards lower contact angles with increasing temperature. Sessile drop measurements by Nakashima [22] evaluated the wetting of 99.999% pure copper on 99.99% pure niobium foil at 1150°C in vacuum. The results indicated an initial contact angle of 67°, which decreased to ≈40° in 5-10 min, and decreased more slowly to ≈28° after 4 h at 1150°C. The initial contact angle values are similar to those reported by DeLima *et al.* [75]; the long-time contact angle is significantly lower. Collectively, the results indicate that contact angles are acute, and decrease with decreasing oxygen content in niobium,▼ increasing temperature, and increasing time at temperature.

Experimental Procedure

Joints were produced by coating alumina with a relatively thin copper layer, inserting a thicker niobium foil between the coated surfaces, and processing the resulting sandwich/assembly in a vacuum hot press at ≈1150°C or ≈1400°C with an applied pressure of ≈2 MPa. Each joined assembly was machined into beams for fracture strength testing. Further characterization of the joints was performed to relate

▼ Unpublished work by Saiz *et al.* [76] has examined the effect of oxygen additions to copper on the wetting behavior. Contact angles near 80° are obtained when 99.999% pure copper is placed on 99.9% pure niobium at 1150°C in gettered argon. If "electronic grade" copper (which contains oxygen) is used instead, then contact angles <20° are obtained. If electronic grade copper is annealed in H_2 prior to the wetting experiment, contact angles close to 60-70° are obtained.

microstructure and processing conditions to the observed strengths. Post-bonding anneals were conducted to explore the effects of temperature and environment on joint stability. Many of the materials and experimental procedures used in this work duplicate those used previously [20, 77].

Materials

The majority of joints fabricated used a 99.5% pure, ≥98% dense alumina (Coors Technical Ceramics Co., Oak Ridge, TN) in the form of 19.5 mm × 19.5 mm × 22.5 mm blocks. Bonding surfaces were ground flat using a surface grinder, then lapped with progressively finer size (9, 6, 3, 1 μm) diamond suspensions (South Bay Technologies, San Clemente, CA), and finished by polishing with a colloidal silica suspension (Struers, Westlake, OH). Some joints were also fabricated using ≈0.5 mm thick, high-purity, optical finish, c-axis (±≈1°) sapphire substrates (Meller Optics Inc., Providence, RI) that required no additional polishing.

Pieces of foil, 20 mm × 23 mm, were cut from a larger sheet of 127 μm thick high-purity (99.99% pure) niobium foil (Goodfellow, Berwyn, PA). The cut foil was pressed and flattened between two steel gauge plates. Afterwards, the foil was washed in a water-detergent mix, given an ultrasonic cleaning in isopropyl alcohol for at least 15 min, rinsed successively in ethanol and nanopure water (minimum 18 MΩ•cm resistivity) and then dried with warm air. A commercial copper wire (Consolidated Companies Wire and Associated, Chicago, IL) used in prior studies served as the copper source.

Coating Procedure

Copper was deposited onto the polished and cleaned alumina substrates by evaporation in a high vacuum chamber. Copper wire pieces were cleaned ultrasonically in isopropyl alcohol for at least 15 min, rinsed in distilled water and bright dipped in a 5:1 nitric acid:water solution for 5-10 s to remove surface oxide. After bright dipping, the copper was immediately rinsed in distilled water and left submerged in isopropyl alcohol. Just prior to loading the deposition system, the copper pieces were rinsed in nanopure water and blown dry with air. Cleaned copper pieces were placed into tungsten wire baskets, and the deposition chamber was then evacuated to $< 2.5 \times 10^{-9}$ atm before heating began. During coating, the chamber pressure ranged from 3×10^{-8} to 3×10^{-7} atm; after coating, the pressure quickly dropped below

2.5×10^{-9} atm. The copper-coated substrates were left in the vacuum deposition chamber until the niobium core layer was cleaned and ready for sample assembly. Film thickness measurements were performed on glass cover slips placed into the chamber during deposition using both step height (profilometry) and weight gain measurements as described previously [20]. The film thickness varies somewhat from sample to sample and with position on a substrate surface. The average thickness is ≈3 μm.

Bonding Conditions and Hot Press

Cleaned niobium foils were placed between copper-coated alumina or sapphire substrates, and loaded into a vacuum hot press. Joints in this study were prepared in a hot press equipped with graphite heating elements, shields, and furniture, that reaches temperatures >1600°C. Prior joining work [20] used a hot press with molybdenum heating elements and shields and alumina furniture; this hot press only reaches ≈1200°C.[✠] The temperature was increased at 4°C/min, however, occasionally the heating cycle had to be interrupted in order to maintain the vacuum below 1.3×10^{-7} atm. Joints were processed at ≈1150°C or ≈1400°C for 6 h under high vacuum with the applied pressure set at the minimum values possible in the two hot presses. Pressures were applied at the onset of heating and maintained. Samples were cooled at 2°C/min. More detailed information is summarized in Table 1.

Beam Preparation

The as-processed blocks were machined into rectangular beams, ≈3 mm × ≈3 mm in cross section and ≈4 cm in length, with the metal interlayer at the beam center. The joined block assembly was first cut into plates, one face of which was ground flat and polished, generally to a 1 μm finish; details are available elsewhere [77]. The polished plates were subsequently cut into beams. The tensile edges of flexure beams were beveled on a 6 μm grinding plate to remove machining flaws that could initiate failure. Subsequently, beams were successively cleaned with acetone, soap and water, and isopropyl alcohol. Just prior to mechanical testing, the beams were cleaned ultrasonically in a denatured HPLC grade ethanol (Aldrich Chemical Company Inc., Milwaukee, WI) and blown dry with warm air. This process primarily serves to remove water trapped in the pores of the ceramic.

[✠] The "graphite" hot press is expected to provide a lower oxygen partial pressure environment during bonding.

Post-bonding Heat Treatments

In order to investigate the effect of prolonged anneals at elevated temperature and differing oxygen partial pressures on beam strength and microstructure, beams which had been beveled and cleaned were placed inside an alumina crucible, heated at 30°C/min and annealed at 1000°C for various lengths of time. Anneals in gettered argon were performed in a furnace with molybdenum heating elements and shields; vacuum anneals were performed in a furnace with tungsten heating elements and molybdenum shields.

For the gettered argon anneals, the argon flows through two tube furnaces prior to entering the annealing furnace, The first is held at ≈40°C and contains anhydrous calcium sulfate (W. A. Hammond Drierite Co., Xenia, OH) which removes excess water vapor from the argon. The second tube furnace contains titanium and zirconium chips at ≈800°C which react with oxygen in the argon. Assuming that equilibrium is reached at 800°C, a p_{O_2} of the order of 10^{-44} atm is predicted. This p_{O_2} would be sufficient to reduce alumina, and thus, a higher p_{O_2} is expected to prevail during anneals at 1000°C. If the p_{O_2} is dictated by aluminum-alumina equilibrium, one expects a p_{O_2} of the order of 10^{-34} atm. This p_{O_2} and the flow rates are sufficiently low that material losses even after anneals of 200 h duration would be immeasurably small.

During the high vacuum anneals, the total pressure was typically $<7 \times 10^{-8}$ atm during heating and fell below 10^{-8} atm after a short time at the annealing temperature. For longer anneals, the total pressure was in the 10^{-10} atm range for much of the duration. At 1000°C, the equilibrium oxygen partial pressure for tungsten-tugnsten oxide and molybdenum-molybdenum oxide equilibrium are comparable (≈10^{-15} atm). This pressure would be sufficiently low to reduce cuprous oxide and copper aluminate, but exceeds the equilibrium p_{O_2} for niobium-niobium oxide equilibrium (≈10^{-25} atm at 1000°C). Thus, some oxidation of niobium may occur during annealing to reduce the ambient p_{O_2}.

Mechanical Testing

Room Temperature

Beams were tested at room temperature using four-point bending. The inner and outer spans were 9 and 25 mm, respectively. Testing was done with a displacement rate of 50 μm/min. Strengths were calculated from the load at failure using standard relationships derived for monolithic elastic materials, *i.e.*,

no correction for stress concentrations arising from modulus misfit [78, 79] was attempted. Prior work had determined that under identical testing conditions, the average four-point bend strength of (unbonded and unannealed) alumina beams prepared from the same source material using similar cutting and polishing procedures is ≈280 MPa [18].

High Temperature

For high-temperature bend tests, beams were loaded into a graphite testing jig situated between a graphite ram assembly in a tungsten heating element furnace. Inner and outer spans were again 9 and 25 mm, respectively. The furnace chamber was evacuated and backfilled with argon which flows during heating, mechanical testing, and cooling of the sample. Typically, samples were heated to (and cooled from) the test temperature at 10°C/min, and held for at least 15 min at the test temperature prior to load application to thermally equilibrate the sample. Rams were displaced at 60 μm/min and the load versus displacement data was exported to a computer data acquisition system.

Microstructural Characterization

In prior work [20], bonds were fabricated at 1150°C, and fracture proceeded primarily along one ceramic-metal interface. Fractographic analysis of such interfaces was reported previously [20]. The majority of the fractures in as-bonded samples prepared at 1400°C were ceramic failures. For selected samples in which failure was interfacial, beam fracture surfaces were mounted adjacent to one another so that equivalent fractographic locations were in mirror symmetry positions. The general microstructure at matching locations, the pore structure, and the fracture path could thus be readily identified. Fracture surfaces were first inspected using optical microscopy, and then examined using scanning electron microscopy (SEM).

For bonds prepared using sapphire substrates, the sapphire/interlayer interfacial microstructure was examined using optical microscopy. Samples were examined both in the as-processed state and after prolonged periods of post-bonding anneal. The evolution of microstructure at specific locations along the interface could be assessed by comparing images taken before and after annealing.

Results and Discussion

Effect of Processing Conditions on Room-Temperature Mechanical Properties

Prior room-temperature strength measurements [20] for alumina joined with a bonding pressure of ≈5.1 MPa at 1150°C in a molybdenum element hot press are summarized and compared to the strength characteristics of the unbonded reference alumina in Figure 1. The average flexure strengths of these as-bonded samples was ≈180 MPa with a standard deviation of ≈25 MPa, and provides a basis for comparison.

The joint strengths obtained for a sample bonded at 1150°C in a graphite element hot press and a more modest bonding pressure of 2.2 MPa are shown in Figure 1. It is clear that the average strength has decreased (80 MPa). All beams that survived the sample preparation procedures suffered interfacial failure. In addition, three of six plates failed during machining/handling of the bonded block, suggesting that the strength variation is even more severe than indicated. Either the reduced p_{O_2} or the reduced bonding pressure, or the combination of both results in substantial strength degradation.

Increasing the bonding temperature to 1400°C, while maintaining the applied load (2.2 MPa) and other parameters, improves the bond properties dramatically. In all three bonds prepared using these conditions, reproducibly high strengths were obtained. The strength results appear as one data set in Figure 1; the average strength is 240 MPa with a standard deviation of 20 MPa. In room temperature bend tests, 25 samples failed entirely in the ceramic, failure in 6 initiated in the ceramic, and the remaining 11 failed along the interface. This suggests that there is a substantial change in the nature of the alumina/interlayer microstructure or adhesion, or both, as a result of the increase in bonding temperature. Copper segregation to the alumina/niobium interface is expected, but does not appear to have a strong adverse effect.

When the fracture surfaces of polycrystalline alumina samples bonded at 1150°C in molybdenum and graphite hot presses are compared, good ceramic-metal contact is indicated in both. There are few obvious interfacial flaws (unbonded regions), and the imprint of the ceramic microstructure is evident on the metal side of failed beams. Thus, the degree of ceramic-metal contact does not appear to cause the

strength difference. What is apparent is that the samples processed in graphite have a significantly higher area fraction of copper, and thus, copper/alumina contact along the interface.

To examine whether this was due to the difference in bonding pressure or to the difference in the ambient p_{O_2}, sapphire-based bonds were prepared in the graphite hot press at 1150°C using bonding pressures of 1.6 and 5.0 MPa. Optical microscopy was used to examine the interface microstructure. In both samples regions were evident in which the copper film remained continuous, and regions could be found in which the film had broken up. A qualitative assessment suggests that the increase in bonding pressure leads to somewhat more breakup of the film, however, the difference is not dramatic. Moreover, the microstructure is quite inhomogeneous. It is possible that microstructural features at an interface with polycrystalline alumina have an important effect on the evolution. Bonds using polycrystalline alumina blocks are being prepared using a 5.0 MPa bonding pressure to see whether fracture strengths and fracture surface microstructures are then more similar to those observed in the original bonds prepared in the molybdenum hot press. It is possible that the greater area fraction of copper/sapphire interfaces, rapid diffusion of oxygen through a continuous copper liquid film, and a low ambient p_{O_2} combine to produce low strengths in joints prepared using low bonding pressures in a graphite hot press.[✧]

Several factors could in principle contribute to the substantial improvement in joint properties that accompanies an increase of the bonding temperature to 1400°C. Temperature-induced changes in the alumina/interlayer microstructure could in principle be the result of changes in the amount of liquid formed, and its wetting behavior, or in the kinetics of morphological evolution.

Increasing the amount of liquid could facilitate the filling of interfacial voids. The copper-niobium phase diagram [50] is a simple eutectic ($T_{eut} \approx 1080$°C), and the liquidus is nearly vertical up to ≈1600°C. At 1150°C, the niobium-saturated liquid contains ≈0.7 at% niobium while at 1400°C it contains ≈1.7 at% niobium. As a result, the difference in the amount of liquid formed at 1150°C versus 1400°C is negligible.

[✧] Although equilibration with a low ambient p_{O_2} could reduce the strength of copper/alumina interfaces, the equilibrium concentration of dissolved oxygen in copper is orders of magnitude lower than that in niobium at constant oxygen potential. Thus, under most conditions niobium would "getter" oxygen from copper. Diffusion of oxygen into niobium involves a much shorter diffusion distance (≈65 μm) than diffusion of oxygen to the external surface (up to ≈1 cm).

To fill interfacial voids and redistribute the niobium-saturated copper liquid film, it is necessary for $(\theta_1 + \theta_2) \leq 180°$, where θ_1 and θ_2 are the contact angles for the liquid on the ceramic and metal, respectively. Prior work has demonstrated that for copper-niobium liquids on alumina, $\theta_1 \leq 114°$ after short times, and decreases with increasing time [22]. Even the short-term value for θ_1, requires only that $\theta_2 \leq 66°$ to satisfy $(\theta_1 + \theta_2) \leq 180°$. Contact angle measurements [75] suggest that $\theta_2 \leq 66°$ for copper-niobium at 1150°C unless the niobium contains >1.5 at% oxygen and $\theta_2 > 64°$. However, there is no reason to expect such high oxygen levels in the present experiments; the wetting studies of Nakashima [22] and the present joining studies used niobium foil from the same source and lot. Since θ_2 in the copper-niobium system decreases significantly with increasing temperature and time, the condition $(\theta_1 + \theta_2) < 180°$ would certainly be met at 1400°C, and a greater driving force for liquid redistribution would be expected. Although more rapid redistribution would be desirable in PTLP bonding where isothermal solidification can occur, this is not an issue in the present system. Moreover, since good ceramic-metal contact and few interfacial defects were evident in samples prepared at 1150°C in graphite, it seems unlikely that the significant improvement in the strength of joints prepared at 1400°C is due purely to improved wetting.

Fracture surfaces of the (few and generally weaker) beams that failed along the interface and studies of interfacial microstructures in sapphire-based bonds prepared at 1400°C (*to be discussed shortly*) indicate that at the higher temperature, breakup of the copper film into discrete particles occurs more rapidly than at 1150°C. Although the interfacial microstructures are similar to those obtained at lower temperature and higher bonding pressure in a molybdenum hot press [20], the joint properties are not. The increased temperature results in a clear improvement in properties, the underlying cause of which is not yet fully understood.

INTERFACIAL MICROSTRUCTURE EVOLUTION

Samples bonded at 1150°C in a molybdenum-element hot press failed primarily along the interface, and this permitted examination of the ceramic/interlayer interface structure. Extensive redistribution of the copper-rich liquid, and the formation of isolated particles of copper along the interface were evident [20]. In

the current study, two bonds were prepared at 1400°C using c-axis sapphire so that the nature of the interface microstructure could be assessed.

Figure 2 shows a series of optical micrographs taken at different locations along the interface of an as-processed joint. The micrographs suggest a sequence of evolution in which niobium/sapphire contact is first achieved along the niobium grain boundaries, Figure 2a, somewhat reminiscent of the findings of Reimanis [52]. In the present case, this is most likely due to the formation of grain boundary grooves as the copper dissolves niobium and "etches" the grain boundary, and the formation of flanking grain boundary groove ridges. De Lima *et al.* [75] provide evidence of preferential (diffusional) penetration of copper along niobium grain boundaries, and report that the major dissolution of the niobium also occurred along the grain boundary. The grain boundary ridges will contact the sapphire, and localized liquid-phase assisted growth of a niobium/sapphire contact zone ensues. When the niobium/sapphire contact area is small, and the bonding load is amplified, deformation of the niobium may contribute to contact growth. One can anticipate that transport of niobium within the niobium-saturated copper liquid will be rapid. When ridge-sapphire contact is complete around the perimeter of a given grain, a thin layer of niobium-saturated copper liquid is isolated atop the grain. Growth of the contact zone leads to regression of this liquid layer towards the grain center. Consistent with observations by Hodkin *et al.* [51], the copper/ niobium interface is not facetted, and thus, the morphology differs from that observed during pore removal [52]. Capillary instabilities reminiscent of those in high-temperature crack healing and in the breakup of thin (solid) metal films on ceramic substrates occur along the edges of the liquid, resulting in the formation of "cylindrical" ligaments of copper-rich liquid along the interface, Figure 2b. These ligaments subsequently appear to undergo Rayleigh instabilities, resulting in the formation of isolated copper droplets at the interface, as shown in Figure 2c.

Neither the substrate nor the foil are perfectly flat. Although the deviations from planarity may be small in an absolute sense, contact between these nonplanar surfaces will create local points of contact and thereby potentially substantial variations in the liquid film thickness. Spatial variations in the liquid film thickness, in tandem with the polycrystalline nature of the niobium foil are believed to contribute to the substantial spatial variability in the microstructure. The grain boundary misorientation varies from grain-

to-grain, causing a spatial variation in the grain boundary groove angle and grooving kinetics. Variations in the liquid film thickness can induce variations in the ridge height that must be achieved to initiate niobium-sapphire contact. Unless the foil is strongly textured, each exposed niobium grain surface will have a different orientation and this will cause grain-to-grain variations in θ_2. As a result, it is not surprising that substantial variations in the microstructure are evident. When polycrystalline alumina substrates are used instead of sapphire, defects in the ceramic surface, grain-to-grain variations in the alumina surface orientation and alumina grain boundary groove characteristics can all be important, and may reduce the spatial scale of variability in microstructural evolution.

High temperature strength and failure mode

The microstructural observations on sapphire/interlayer couples suggest that over a substantial fraction of the sapphire/interlayer interface, niobium is in contact with sapphire. The room-temperature fracture results for samples bonded at 1400°C show highly reproducible strengths. As a result, a limited number of beams from samples bonded at 1400°C were subjected to short-time elevated temperature bend tests in an argon atmosphere.

The test results are summarized in Figure 3. Five beams from this sample were tested at room temperature. Four failed in the ceramic; in a fifth, failure initiated within the ceramic, but the crack was drawn to the interface. The average room temperature strength from this subset was of the order 245 MPa, consistent with the larger set of data from bonds prepared at 1400°C. Average strengths >200 MPa are retained to temperatures of 900°C, with the lowest strengths corresponding to interfacial failures, and at 1100°C, a bend strength of ≈85 MPa is observed. Even allowing for a ±20°C error in the temperature measurement, this test temperature is above 99% of the melting point of copper. This observation does suggest that substantial niobium/alumina bonding is achieved, and argues against the existence of a very thin residual copper layer along the interface. Perhaps most striking about the results is that many of the failures (*see insert in Figure 3*) occur within the ceramic and thus, the observed strength decrease appears to reflect the characteristics of the alumina, not of the joint itself. (Presumably, the strength decrease is the result of a small amount of glassy phase in this alumina.)

Effect of post-bonding heat treatments on room temperature strength

The potentially important effect of the ambient oxygen partial pressure on near-interfacial chemistry in niobium/alumina(sapphire) bonds has been discussed in numerous publications [e.g., 29-31, 38, 39, 42, 46, 47, 80, 81]. The high-temperature mechanical tests may be of too short a duration for any substantial adjustment of the interface chemistry to occur over a spatial scale that would affect failure. In a prior study [20], bonds fabricated at 1150°C in a molybdenum hot press were subjected to 10 h anneals at 1000°C in gettered argon, and retested at room temperature. The results suggested a possible improvement in strength, however, due to other factors, a definitive conclusion was not possible. In subsequent experiments, samples processed at 1400°C were subjected to 5 h and 50 h gettered argon anneals at 1000°C, and retested at room temperature. Although a 5 h anneal had no discernable effect, there appeared to be a strength drop after a 50 h anneal. A more complete investigation of this behavior was pursued, both to explore potential effects of prolonged high temperature exposure on strength, and to see whether any evidence could be obtained for an effect of oxygen partial pressure on strength characteristics.

Figure 4 summarizes the results of room temperature strength tests after beams processed at 1400°C were annealed for periods of 0, 5, 50, 200, and 220 h at 1000°C in gettered argon. Beams tested in the as-processed state had an average fracture strength of 240 MPa, and ceramic failures outnumber interfacial failures by a roughly 3:1 ratio. A single sample annealed for 5 h failed in the ceramic at a stress of ≈240 MPa. An increase in the anneal time to 50 h results in a decrease in the mean strength to ≈210 MPa, with ceramic and interfacial failures still in a 3:1 ratio. When anneal times are increased to 200 or 220 h, the mean strength is again somewhat less than that of as-processed samples. Although a least squares fit of the strength data does suggest a decline in strength with increasing anneal time, the decrease is modest. What is perhaps more significant is that all failures in this set occurred along the interface. The likelihood that all five samples annealed for ≥200 h would fail along the interface in the absence of some microstructural or microchemical change seems remote.

To explore whether the observed changes in fracture strength were the result of a microstructural or microchemical change that was purely the result of prolonged annealing, bend beams were also annealed for 200 h at 1000°C in a vacuum environment. Four beams failed at an average strength of 225 MPa, and

three of four beams failed in the ceramic, as shown in Figure 4. Sapphire couples were also annealed for 200 h, and the microstructures of the same areas at the interface compared. As shown in Figure 5, there is no discernable change in the interfacial microstructure; this also supports the view that the extensive microstructural adjustments that occur during bonding are facilitated by niobium diffusion within the copper-rich liquid. Such prolonged anneals should also allow for copper dissolved in the near-interfacial region to segregate to the interface. There is no substantial strength loss and no obvious shift in fracture path when samples are annealed in vacuum.

In an effort to understand the different fracture path tendencies, the fracture surfaces of (the one) vacuum annealed and the argon annealed beams that failed along the interface were compared. In Figure 6, four micrographs are presented. The left-hand column shows the ceramic (*top*) and metal (*bottom*) side of the fracture surface of a vacuum-annealed sample. The tensile edge of the beam lies at the common edge of the micrographs, and thus equivalent positions are situated at equivalent distances from the common edge. One notes that the ceramic grain structure, clearly evident in the top micrograph, is "reflected" across this edge, implying good ceramic-metal contact, and that grain boundary grooves formed in the alumina cause corresponding features, presumably ridges, on the niobium surface. The failure proceeds through the copper, leaving traces on both sides of the fracture surface. In contrast, the argon-annealed samples show that a microstructurally distinct "reaction product" has formed near the tensile surface, and fracture appears to proceed through this layer. By scanning the tensile edge and adjusting the focus, one concludes that this reaction product lies (or at least extends) on the interlayer side of the original interlayer/alumina interface. The thinness and limited spatial extent of this layer have complicated efforts to determine its nature. EDS measurements indicate the layer contains niobium and aluminum. Since similar results are obtained on the metal fracture surface, one can preclude that the aluminum signal comes from the underlying alumina. Beyond this region, there again appears to be intimate contact between the ceramic and metal as evidenced by the imprint of the alumina grain boundaries on the niobium. Since anneals in very low p_{O_2} environments would deplete the niobium of oxygen and thereby allow higher aluminum concentrations to be reached, the possibility exists that the reaction product is a niobium aluminide (Nb_3Al). The formation

of a particularly brittle intermetallic interphase may facilitate failure initiation along the interface and contribute to the observed change in fracture path. Further tests are in progress.

Summary and Conclusions

The results suggest that processing temperature, bonding pressure and the furnace environment (ambient oxygen partial pressure) can play a key role in defining the strength characteristics of a joined assembly. Polycrystalline aluminas joined using copper/niobium/copper interlayers at 1150°C and 1400°C in a graphite element hot press have dramatically different properties. Similarly, joints prepared at two different bonding pressures at 1150°C exhibit different interfacial microstructures. Although intimate ceramic-metal contact is achieved in both 1150°C bonds, a clear difference in the failure behavior exists. Fracture surfaces of alumina beams and interfacial microstructures in sapphire-based bonds seem to suggest that the strengths increase as the area fraction of niobium/alumina (versus copper/alumina) contact at the interface increases. An increase in the bonding temperature at constant pressure, and to a much lesser degree an increase in pressure at constant bonding temperature appear to lead to more complete "dewetting" of the copper films and more extensive formation of niobium/sapphire contact. Whether the relatively lower p_{O_2} expected in a graphite environment also detrimentally affects the joint properties remains to be confirmed. The joints produced in a graphite hot press at 1400°C are formed at low ambient p_{O_2}, however, they exhibit consistently good room temperature properties.

Additional experiments using sapphire are being conducted to allow a more thorough and quantitative comparison of the interfacial microstructures produced in the two furnace environments at 1150°C, and those produced in graphite at 1150°C and 1400°C. In addition, polycrystalline alumina assemblies are being fabricated in the graphite hot press at 1150°C with a higher joining pressure and will be tested to isolate the effect of bonding pressure on fracture characteristics.

The high fraction of ceramic failures in "optimized" joints implies that further improvements in strength, and perhaps an even higher frequency of ceramic failure could be achieved with an alumina of

higher strength and an improved microstructure. Preliminary room-temperature strength results on bonds produced using a higher-strength higher-purity commercial alumina support this contention [82].

The observation that reasonable strengths could be maintained to temperatures beyond those accessible with conventional brazes (*e.g.*, Cusil ABA™) is encouraging. It suggests that the use of multilayer interlayers in which thin liquid-forming layers undergo similar morphological changes may provide a new means of producing joints that are useful at elevated temperatures. Since the phase diagram and kinetic considerations in selecting such liquid formers differ from those for PTLP bonding, this may provide additional options for interlayer design. Since high-temperature strengths were often limited by the properties of the ceramic it may be possible to further improve the strength-temperature characteristics of such joints, and to extend the utility of the joint to higher temperatures than presently demonstrated.

Finally, the results indicate that prolonged high-temperature anneals in a low p_{O_2} ambient can have an adverse effect on joint performance. Both the vacuum and gettered argon anneals involve p_{O_2} values well below those required to oxidize copper or to form copper aluminates, and as a result, copper-based interphases are not expected to play a role in the present studies. As would be expected on thermodynamic grounds, interphases were not evident in as-bonded sapphire couples even in regions of extensive sapphire/copper contact. Although anneals in vacuum produce no obvious microstructural changes, anneals in gettered argon produce what appears to be a reaction layer or interphase along the ceramic/interlayer interface near the external surface. The nature of this reaction layer needs to be identified. One can speculate that if the thin reaction layer is mechanically weak it may provide a preferred site for failure initiation, and that once initiated near the ceramic/interlayer interface failure simply proceeds along the ceramic/interlayer interface. An alternative explanation is that prolonged exposure to a low p_{O_2} environment induces a more extensive change in the ceramic/interlayer chemistry that affects the adhesion and thereby the fracture path. Further work will be required to resolve this issue.

Acknowledgements

This research was supported by the Director, the Office of Energy Research, Office of Basic Energy Sciences, Materials Sciences Division of the U.S. Department of Energy under Contract No. DE-AC03-76SF00098. The authors thanks Rowland Cannon, Ivar Reimanis, Eduardo Saiz, Mark Sixta and Tony Tomsia for helpful discussions, experimental assistance, and access to unpublished research results.

References

[1] M. G. Nicholas and D. A. Mortimer, *Mater. Sci. Tech.*, **1**, [9], 657-65 (1985).

[2] K. Suganuma, Y. Miyamoto, and M. Koizumi, *Ann. Rev. Mater. Sci.*, **18**, 47-33 (1988).

[3] R. E. Loehman and A. P. Tomsia, *Am. Ceram. Soc. Bull.*, **67**, [2], 375-80 (1988).

[4] G. Elssner and G. Petzow, *ISIJ Int.*, **30**, [12], 1011-1032 (1990).

[5] M. G. Nicholas, Joining of ceramics, 1st ed. London ; New York: Published on behalf of the Institute of Ceramics by Chapman and Hall, 1990.

[6] R. E. Loehman, in Surfaces and interfaces in ceramic and ceramic-metal systems, J. A. Pask and A. G. Evans, Eds. New York: Plenum Press, 1981, pp. 701-711.

[7] R. D. Brittain, S. M. Johnson, R. H. Lamoreaux, and D. J. Rowcliffe, *J. Am. Ceram. Soc.*, **67**, [8], 522-6 (1984).

[8] M. L. Mecartney, R. Sinclair, and R. E. Loehman, *J. Am. Ceram. Soc.*, **68**, [9], 472-8 (1985).

[9] S. M. Johnson and D. J. Rowcliffe, *J. Am. Ceram. Soc.*, **68**, [9], 468-72 (1985).

[10] S. Baik and R. Raj, *J. Am. Ceram. Soc.*, **70**, [5], C105-7 (1987).

[11] P. A. Walls and M. Ueki, *J. Am. Ceram. Soc.*, **78**, [4], 999-1005 (1995).

[12] M. Gopal, L. C. De Jonghe, and G. Thomas, *Acta Mater.*, **46**, [7], 2401-5 (1998).

[13] S. J. Glass, F. M. Mahoney, B. Quillan, J. P. Pollinger, and R. E. Loehman, *Acta Mater.*, **46**, [7], 2393-9 (1998).

[14] T. Iseki, K. Yamashita, and H. Suzuki, *Proc. Brit. Ceram. Soc.*, **31**, 1-8 (1981).

[15] T. Iseki, K. Yamashita, and H. Suzuki, *J. Am. Ceram. Soc.*, **64**, [1], C13-14 (1981).

[16] Y. Iino and N. Taguchi, *J. Mater. Sci. Lett.*, **7**, [9], 981-2 (1988).

[17] Y. Iino, *J. Mater. Sci. Lett.*, **10**, [2], 104-6 (1991).

[18] M. L. Shalz, B. J. Dalgleish, A. P. Tomsia, and A. M. Glaeser, *J. Mater. Sci.*, **28**, [6], 1673-84 (1993).

[19] M. L. Shalz, B. J. Dalgleish, A. P. Tomsia, and A. M. Glaeser, *J. Mater. Sci.*, **29**, [12], 3200-8 (1994).

[20] M. L. Shalz, B. J. Dalgleish, A. P. Tomsia, R. M. Cannon, and A. M. Glaeser, *J. Mater. Sci.*, **29**, [14], 3678-90 (1994).

[21] B. J. Dalgleish, A. P. Tomsia, K. Nakashima, M. R. Locatelli, and A. M. Glaeser, *Scripta Metall. Mater.*, **31**, [8], 1043-8 (1994).

[22] M. R. Locatelli, A. P. Tomsia, K. Nakashima, B. J. Dalgleish, and A. M. Glaeser, *Key Eng. Mater.*, **111-112**, 157-90 (1995).

[23] B. J. Dalgleish, K. Nakashima, M. R. Locatelli, A. P. Tomsia, and A. M. Glaeser, *Ceram. Int.*, **23**, [4], 313-22 (1997).

[24] G. Ceccone, M. G. Nicholas, S. D. Peteves, A. P. Tomsia, B. J. Dalgleish, and A. M. Glaeser, *Acta Mater.*, **44**, [2], 657-67 (1996).

[25] M. Paulasto, G. Ceccone, and S. D. Peteves, *Scripta Mater.*, **36**, [10], 1167-73 (1997).

[26] S. D. Peteves, M. Paulasto, G. Ceccone, and V. Stamos, *Acta Mater.*, **46**, [7], 2407-14 (1998).

[27] S. Morozumi, M. Kikuchi, and T. Nishino, *J. Mater. Sci.*, **16**, [8], 2137-44 (1981).

[28] M. Rühle, K. Burger, and W. Mader, *J. Microsc. Spectrosc. Electron. (France)*, **11**, 163-77 (1986).

[29] G. Elssner and G. Petzow, *Z. Metallkde.*, **64**, [4], 280-86 (1973).

[30] M. Rühle, M. Backhaus-Ricoult, K. Burger, and W. Mader, in Ceramic Microstructures '86, J. A. Pask and A. G. Evans, Eds. New York: Plenum Press, 1987, pp. 295-305.

[31] K. Burger, W. Mader, and M. Rühle, *Ultramicroscopy*, **22**, 1-13 (1987).

[32] H. F. Fischmeister, W. Mader, B. Gibbesch, and G. Elssner, in Interfacial structure, properties, and design, vol. 122, *Mat. Res. Soc. Proc.*, W. A. T. Clark, C. L. Briant, and M. H. Yoo, Eds. Pittsburgh, Pa.: Materials Research Society, 1988, pp. 529-540.

[33] B. Gibbesch and G. Elssner, *Acta Metall. Mater.*, **40**, [Supplement], S59-66 (1992).

[34] B. Gibbesch, G. Elssner, W. Mader, and H. Fischmeister, *Ceram. Eng. Sci. Proc.*, **10**, [11-12], 1503-14 (1989).

[35] D. Korn, G. Elssner, H. F. Fischmeister, and M. Rühle, *Acta Metall. Mater.*, **40**, [Supplement], S355-60 (1992).

[36] B. Gibbesch, G. Elssner, W. Mader, and H. F. Fischmeister, in Joining ceramics, glass, and metal, W. Kraft and Deutsche Gesellschaft für Metallkunde, Eds. Oberursel: DGM Informationsgesellschaft, 1989, pp. 65-72.

[37] M. Turwitt, G. Elssner, and G. Petzow, *J. de Physique*, **46**, [Supplement C4], 123-7 (1985).

[38] K. Burger and M. Rühle, *Ceram. Eng. Sci. Proc.*, **10**, [11-12], 1549-1566 (1989).

[39] K. Burger and M. Rühle, *Ultramicroscopy*, **29**, [1-4], 88-97 (1989).

[40] G. Elssner, H. Jehn, and E. Fromm, *High Temp.-High Press.*, **10**, [5], 487-92 (1978).

[41] G. Elssner and G. Hörz, *Z. Metallkde.*, **62**, [3], 217-22 (1971).

[42] G. Elssner, S. Riedel, and R. Pabst, *Prakt. Metall.*, **12**, 234-43 (1975).

[43] R. A. Perkins and R. A. Padgett, Jr., *Acta Metall.*, **25**, [10], 1221-30 (1977).

[44] R. Kirchheim, *Acta Metall.*, **27**, [5], 869-78 (1979).

[45] G. I. Nikolaev and N. V. Bodrov, *Russ. J. Phys. Chem.*, **52**, [6], 821-823 (1978).

[46] M. Backhaus-Ricoult, *Ber. Bunsenges. Phys. Chem.*, **90**, [8], 684-90 (1986).

[47] J. T. Klomp, in Ceramic Microstructures '86, J. A. Pask and A. G. Evans, Eds. New York: Plenum Press, 1987, pp. 307-317.

[48] G. Elssner, D. Korn, and M. Rühle, *Scripta Metall. Mater.*, **31**, [8], 1037-42 (1994).

[49] S. Gerardi, in Metals Handbook, vol. 2, 10th ed. Materials Park, OH: ASM International, 1990, pp. 565-571.

[50] T. B. Massalski, H. Okamoto, and ASM International, Binary alloy phase diagrams, 2nd ed. Materials Park, Ohio: ASM International, 1990.

[51] E. N. Hodkin, M. G. Nicholas, and D. M. Poole, *J. Less-Common Metals*, **20**, [2], 93-103 (1970).

[52] I. E. Reimanis, *Acta Metall. Mater.*, **40**, [Supplement], S67-74 (1992).

[53] C. A. M. Mulder and J. T. Klomp, *J. de Physique*, **46**, [Supplement C4], 111-16 (1985).

[54] R. M. Crispin and M. G. Nicholas, *Ceram. Eng. Sci. Proc.*, **10**, [11-12], 1575-81 (1989).

[55] C. Beraud, M. Courbiere, C. Esnouf, D. Juve, and D. Treheux, *J. Mater. Sci.*, **24**, [12], 4545-54 (1989).

[56] L. Esposito, A. Bellosi, S. Guicciardi, and G. De Portu, *J. Mater. Sci.*, **33**, [7], 1827-36 (1998).

[57] M. Rühle, A. Liedtke, U. Alber, R. Schweinfest, and G. Elssner, in Interfacial Science in Ceramic Joining, A. Bellosi, T. Kosmac, and A. P. Tomsia, Eds.: Kluwer Academic Publishers, Dordrecht, The Netherlands, 1998, pp. 3-14.

[58] B. C. Allen and W. D. Kingery, *Trans. AIME*, **215**, [2], 30-37 (1959).

[59] M. Nicholas, R. R. D. Forgan, and D. M. Poole, *J. Mater. Sci.*, **3**, [1], 9-14 (1968).

[60] A. C. D. Chaklader, A. M. Armstrong, and S. K. Misra, *J. Am. Ceram. Soc.*, **51**, [11], 630-3 (1968).

[61] T. E. O'Brien and A. C. D. Chaklader, *J. Am. Ceram. Soc.*, **57**, [8], 329-32 (1974).

[62] K. Nogi, K. Oishi, and K. Ogino, *Mater. Trans., JIM*, **30**, [2], 137-45 (1989).

[63] P. Nikolopoulos, S. Agathopoulos, and A. Tsoga, *J. Mater. Sci.*, **29**, [16], 4393-8 (1994).

[64] V. Ghetta, J. Fouletier, and D. Chatain, *Acta Mater.*, **44**, [5], 1927-36 (1996).

[65] Y. Yoshino, *J. Am. Ceram. Soc.*, **72**, [8], 1322-7 (1989).

[66] S. T. Kim and C. H. Kim, *J. Mater. Sci.*, **27**, [8], 2061-6 (1992).

[67] C. E. Ransley, *J. Inst. Metals (London)*, **65**, [1], 147-172 (1939).

[68] R. L. Pastorek and R. A. Rapp, *Trans. AIME*, **245**, [8], 1711-1720 (1969).

[69] A. V. Ramana Rao and V. B. Tare, *Z. Metallkde.*, **63**, [2], 70-3 (1972).

[70] J. Orszagh and E. Bouillon, *Memoires Scientifiques de la Revue de Metallurgie*, **70**, [4], 319-25 (1973).

[71] K. A. Rogers, K. P. Trumble, B. J. Dalgleish, and I. E. Reimanis, *J. Am. Ceram. Soc.*, **77**, [8], 2036-42 (1994).

[72] I. E. Reimanis, K. P. Trumble, K. A. Rogers, and B. J. Dalgleish, *J. Am. Ceram. Soc.*, **80**, [2], 424-32 (1997).

[73] C. M. Kennefick and R. Raj, *Acta Metall.*, **37**, [11], 2947-52 (1989).

[74] Q. Guo and P. J. Moller, *Surface Science*, **244**, [3], 228-36 (1991).

[75] O. F. De Lima, M. Krehl, and K. Schulze, *J. Mater. Sci.*, **20**, [7], 2464-70 (1985).

[76] E. Saiz, R. M. Cannon, and A. P. Tomsia, unpublished research, 1998.

[77] R. A. Marks, M.S. Thesis, Department of Materials Science and Mineral Engineering, University of California, Berkeley, (2000).

[78] B. J. Dalgleish, M. C. Lu, and A. G. Evans, *Acta Metall.*, **36**, [8], 2029-35 (1988).

[79] H. C. Cao, M. D. Thouless, and A. G. Evans, *Acta Metall.*, **36**, [8], 2037-46 (1988).

[80] D. Knauss and W. Mader, *Ultramicroscopy*, **37**, [1-4], 247-62 (1991).

[81] W. Mader and M. Ruhle, *Acta Metall.*, **37**, [3], 853-66 (1989).

[82] R. A. Marks, unpublished research, 1999.

Tables

Table 1: Summary of Processing Conditions for Each Joint

Substrate	Hot Press	Joining Temperature (°C)	Applied Load (MPa)	Holds (°C-min)
Coors alumina	graphite	1394	2.2	none
Coors alumina	graphite	1150	2.2	none
Coors alumina	graphite	1394	2.2	1199-30
Coors alumina	graphite	1394	2.2	1169-56
(0001) sapphire window	graphite	1394	2.9	1108-96 1218-139 1329-111
(0001) sapphire window	graphite	1382	2.2	none

Figure Captions:

Figure 1 Plot of failure probability versus beam fracture strength illustrating effect of processing conditions on joint characteristics. The alumina reference material was unbonded and not annealed prior to testing.

Figure 2 Illustration of interfacial microstructures in a sapphire/copper/niobium couple bonded at 1400°C showing possible sequence for microstructural evolution: a) initial niobium/sapphire contact along grain boundary ridges, b) regression and instability of isolated copper films, and c) regions of largely niobium/sapphire contact with small isolated copper droplets.

Figure 3 Plot of beam fracture strength versus temperature. Strengths are retained to high temperature, and instances of ceramic failure are observed in the 900°C-1100°C test temperature interval. The insert shows examples of some of the higher temperature fractures. Points characterized as interfacial failures correspond to samples in which the failure initiated and propagated entirely along the interface. Points characterized as ceramic failures involve failure entirely within the ceramic. In some cases, the failure initiated in the ceramic, but propagated along the interface; these are designated ceramic to interfacial failures.

Figure 4 Plot of fracture strength versus duration of anneals at 1000°C in gettered argon, or in vacuum. The line is a least squares fit of all gettered argon anneal data. The four strengths measured for samples vacuum-annealed for 200 h were virtually identical; three failures were in the ceramic while one was interfacial. The average value is indicated by an open circle. These data were not included in the fit.

Figure 5 Comparison of interfacial microstructures a) before and b) after 200 h anneal in gettered argon.

Figure 6 Comparison of matching fracture surfaces for beams annealed 200 hat 1000°C. The top and bottom rows correspond to the ceramic and metal sides of the fracture surfaces, respectively. The left-hand and right-hand columns are the argon- and vacuum-annealed samples, respectively. The bottom and top edges of the top and bottom rows of micrographs correspond to the tensile surface, and features “reflect” across this edge. A reaction layer is evident in the argon-annealed sample.

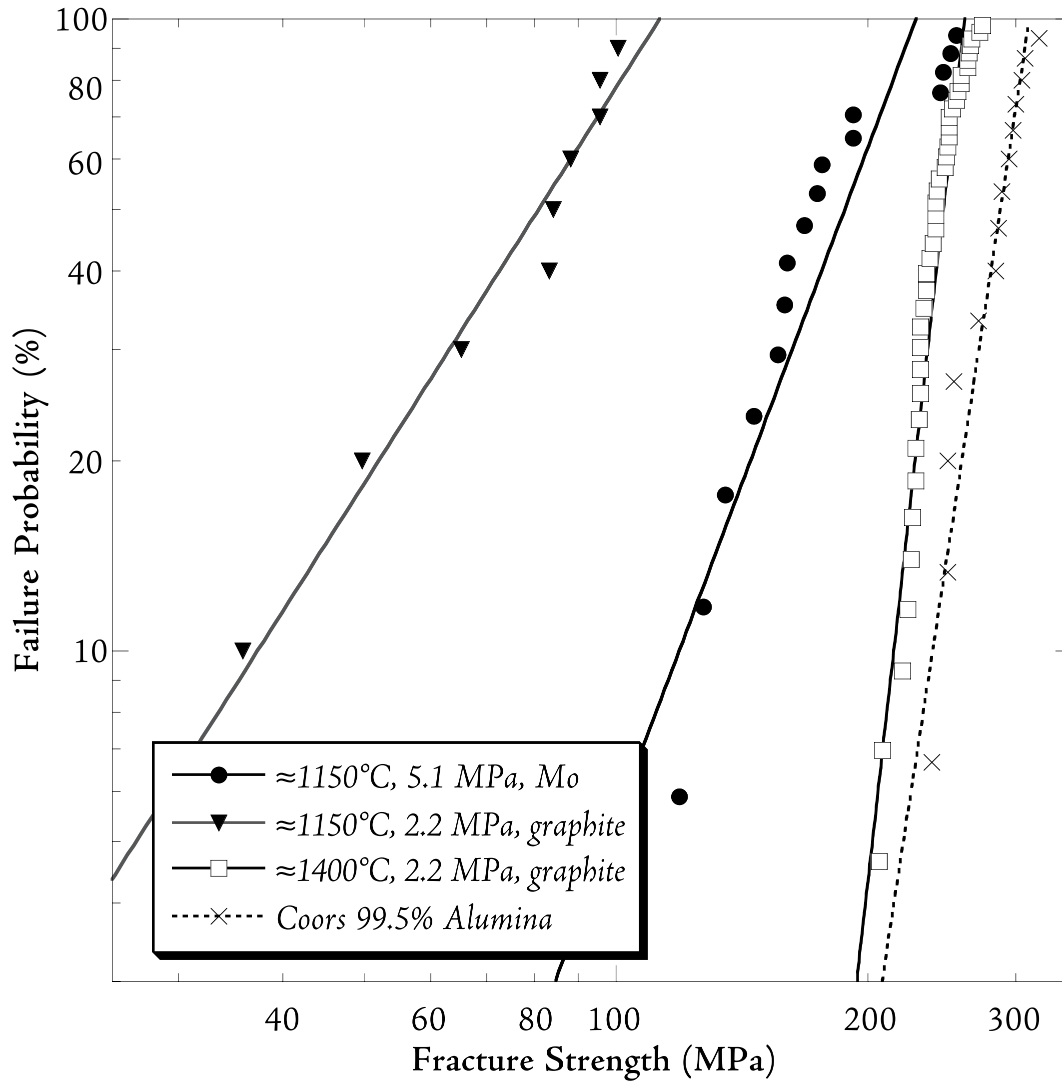

Figure 1 Plot of failure probability versus beam fracture strength illustrating effect of processing conditions on joint characteristics. The alumina reference material was unbonded and not annealed prior to testing.

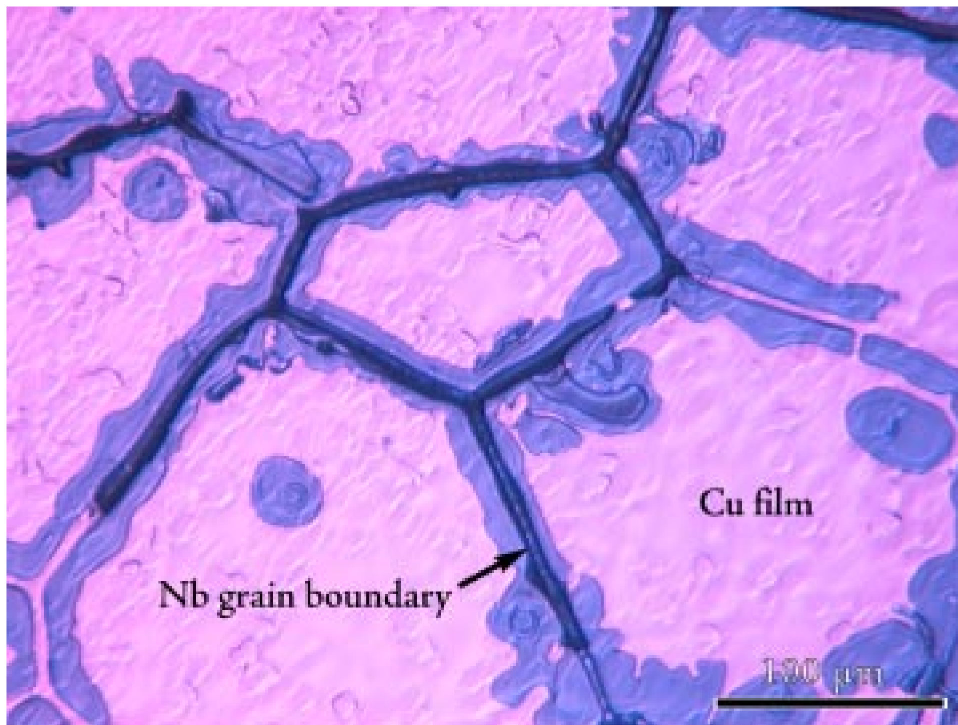

(a)

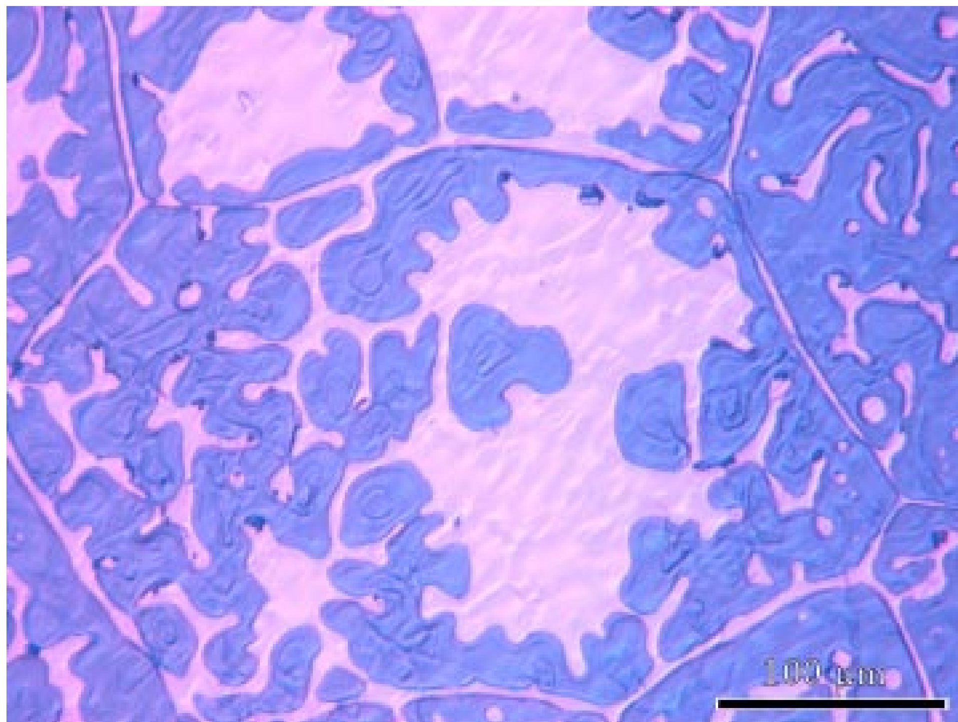

(b)

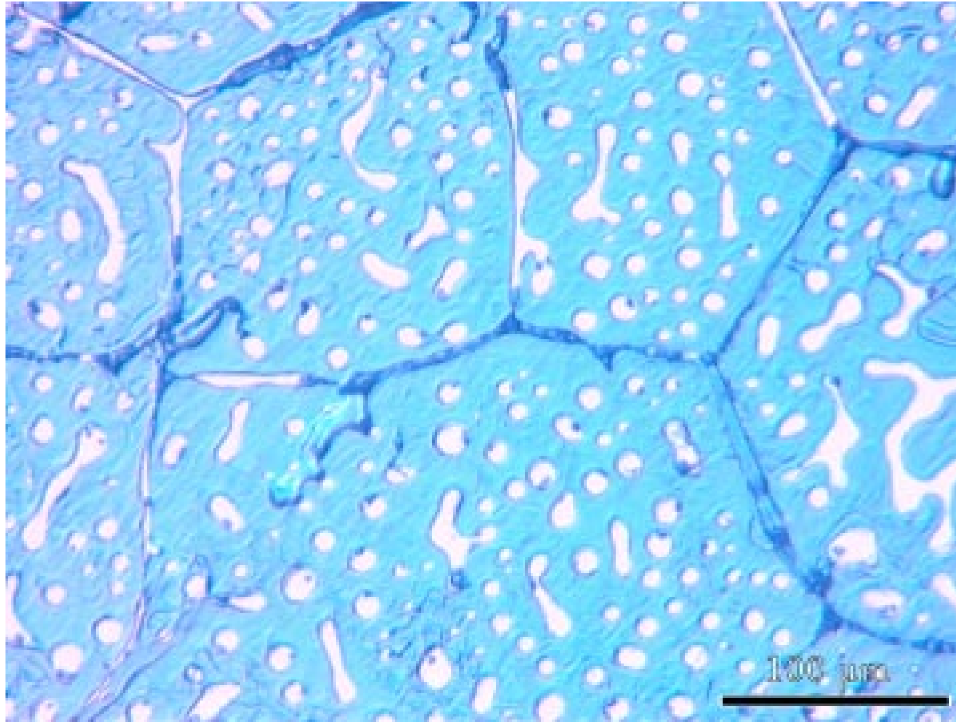

(c)

Figure 2 Illustration of interfacial microstructures in a sapphire/copper/niobium couple bonded at 1400°C showing possible sequence for microstructural evolution: a) initial niobium/sapphire contact along grain boundary ridges, b) regression and instability of isolated copper films, and c) regions of largely niobium/sapphire contact with small isolated copper droplets.

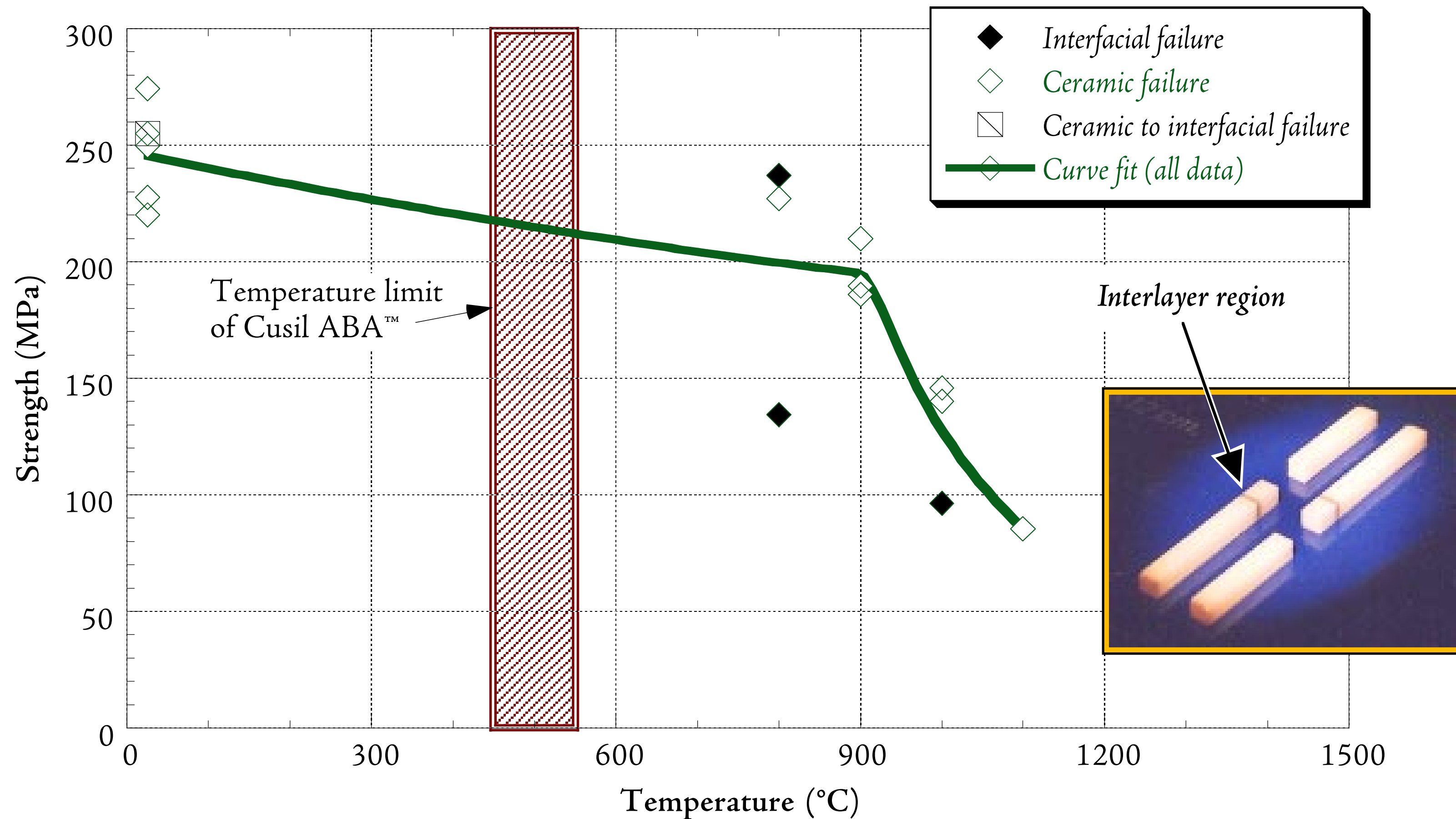

Figure 3 Plot of beam fracture strength versus temperature. Strengths are retained to high temperature, and instances of ceramic failure are observed in the 900°C-1100°C test temperature interval. The insert shows examples of some of the higher temperature fractures. Points characterized as interfacial failures correspond to samples in which the failure initiated and propagated entirely along the interface. Points characterized as ceramic failures involve failure entirely within the ceramic. In some cases, the failure initiated in the ceramic, but propagated along the interface; these are designated ceramic to interfacial failures.

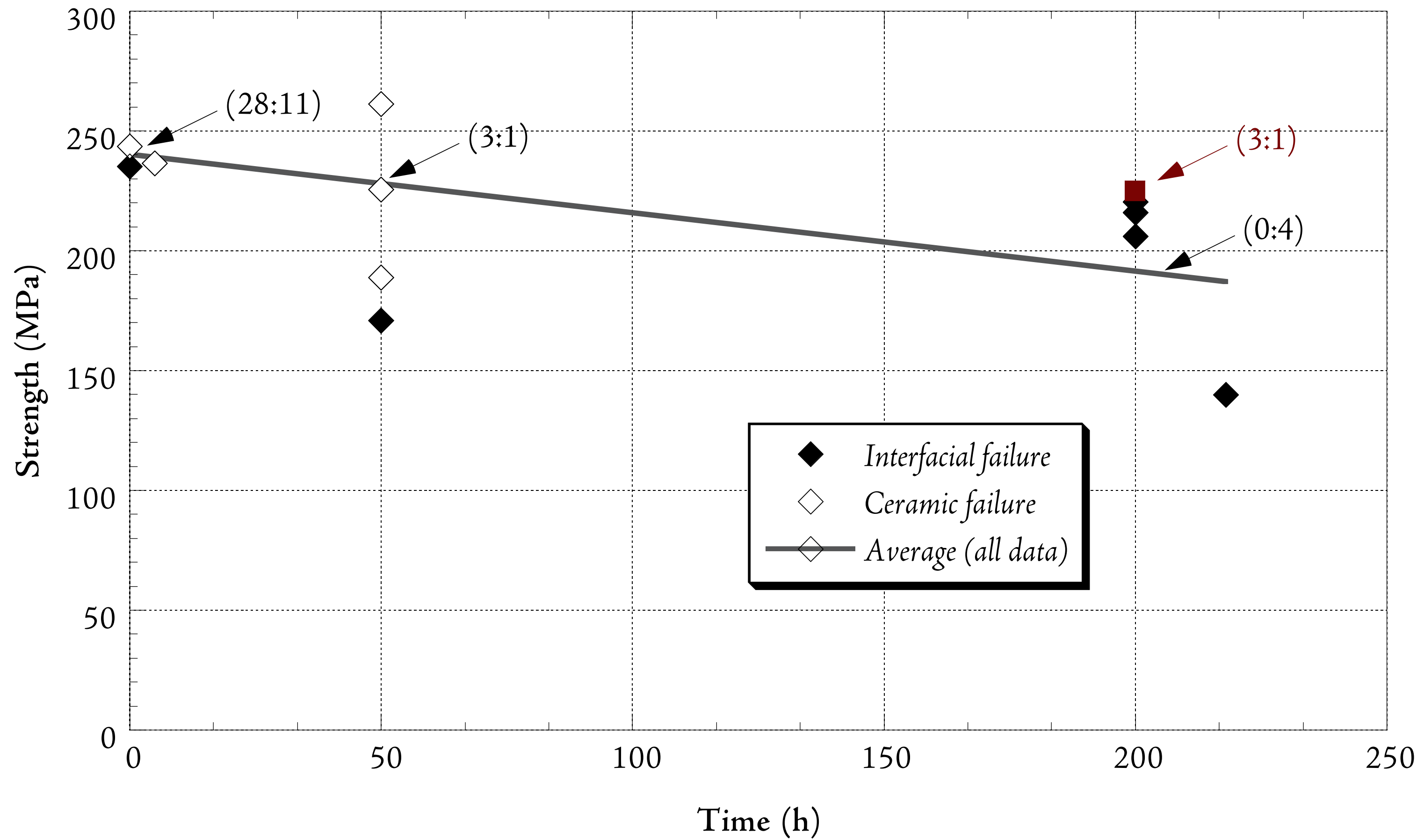

Figure 4 Plot of fracture strength versus duration of anneals at 1000°C in gettered argon, or in vacuum. The line is a least squares fit of all gettered argon anneal data. The four strengths measured for vacuum annealed samples were virtually identical. The average value is indicated in red (■). These data were not included in the fit.

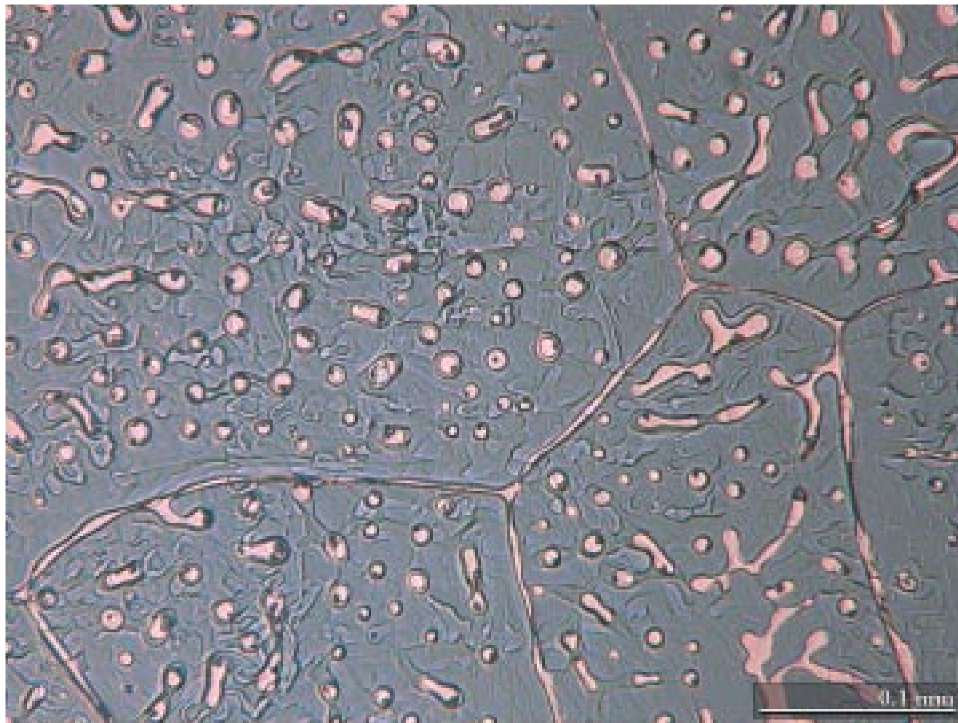

(a)

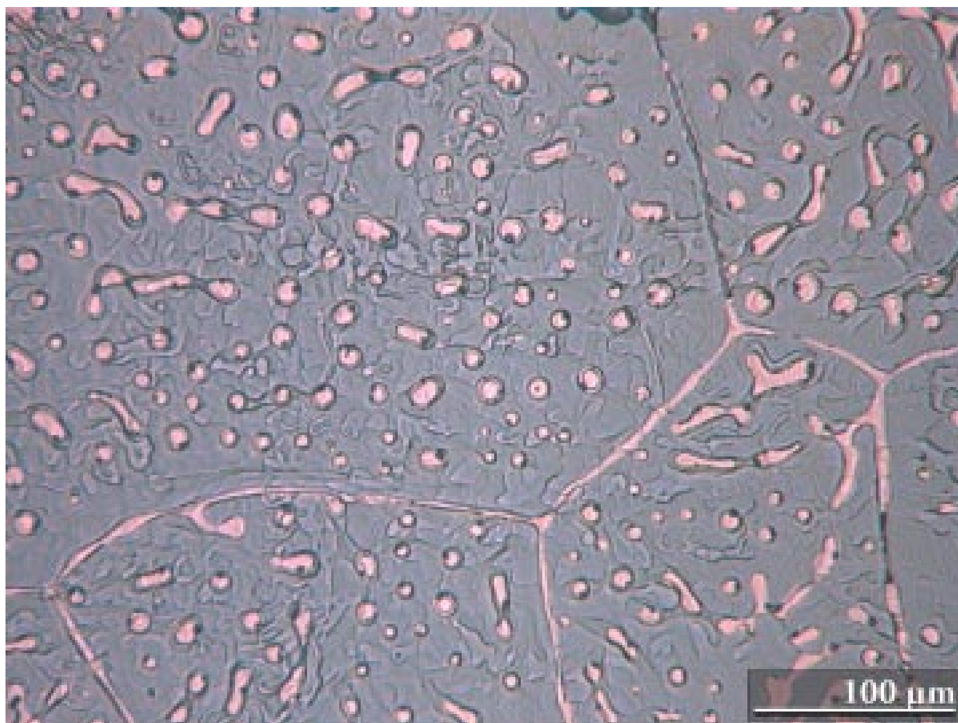

(b)

Figure 5 Comparison of interfacial microstructures a) before and b) after 200 h anneal in gettered argon. Few significant changes are evident.

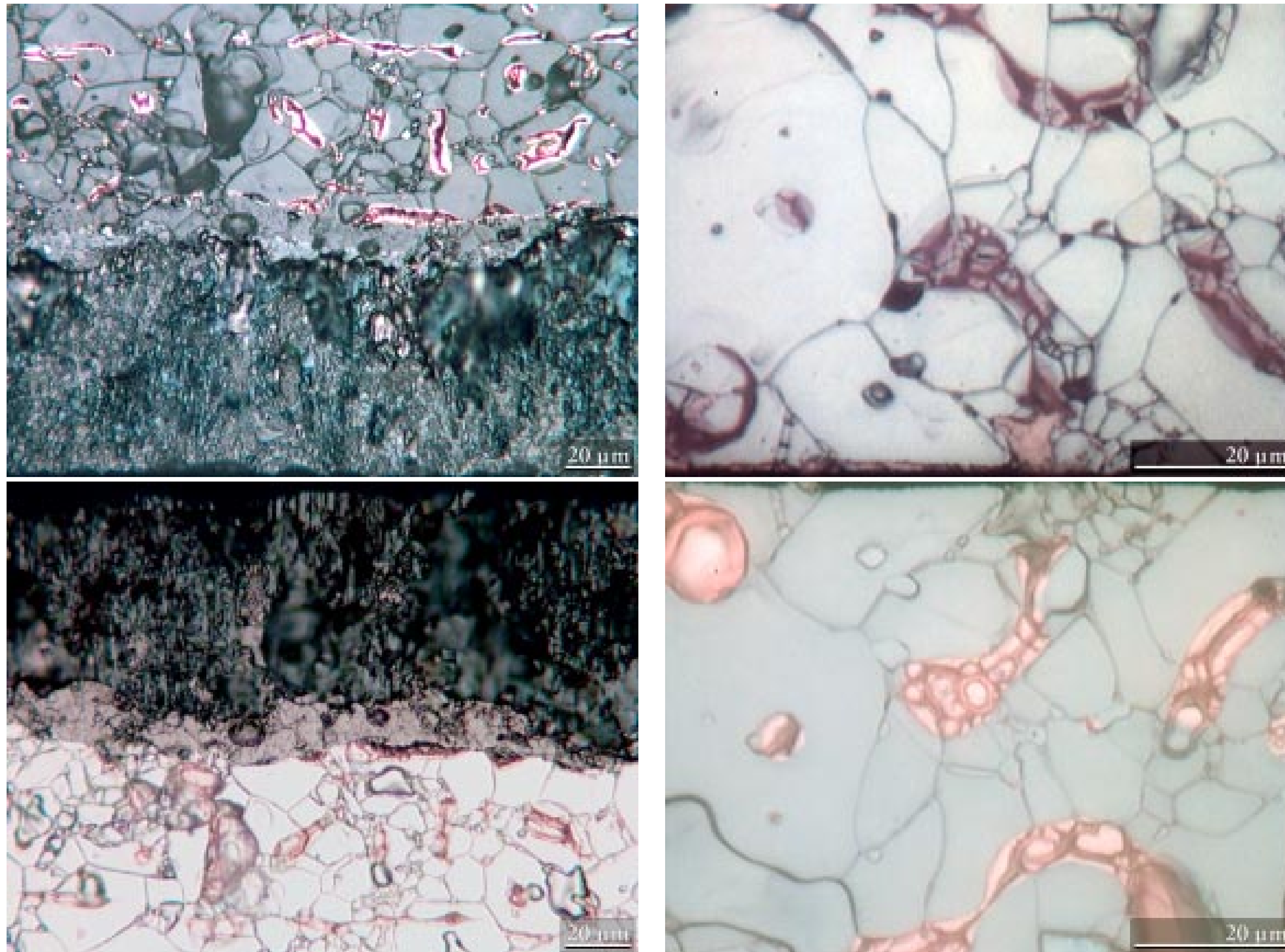

Figure 6 Comparison of matching fracture surfaces for beams annealed 200 h at 1000°C. The top and bottom rows correspond to the ceramic and metal sides of the fracture surfaces, respectively. The left-hand and right-hand columns are the argon- and vacuum-annealed samples, respectively. The bottom and top edges of the top and bottom rows of micrographs correspond to the tensile surface, and features "reflect" across this edge. A reaction layer is evident in the argon-annealed sample.